

Optical surface waves on one-dimensional photonic crystals: investigation of loss mechanisms and demonstration of centimeter-scale propagation

Babak Vosoughi Lahijani,^{1,2,*} Nicolas Descharmes,¹ Raphael Barbey,¹ Gael D. Osowiecki,¹ Valentin J. Wittwer,³ Olga Razskazovskaya,³ Thomas Südmeyer,³ and Hans Peter Herzig¹

¹ Optics & Photonics Technology (OPT) Laboratory, École Polytechnique Fédérale de Lausanne (EPFL), rue de la Maladière 71b, CH-2002 Neuchâtel, Switzerland

²Currently with the Department of Photonics Engineering, DTU Fotonik, Technical University of Denmark, DK-2800 Kgs. Lyngby, Denmark

³Laboratoire Temps-Fréquence, Université de Neuchâtel, Av. de Bellevaux 51, CH-2000 Neuchâtel, Switzerland

Abstract:

It has been predicted that optical surface waves at interfaces that separate purely dielectric media should be able to propagate over long distances, particularly over distances greater than possible with surface plasmon polaritons. Despite numerous studies, there has been no report of such an observation, and an estimate of the propagation length achievable with dielectric optical surface waves is yet to be provided. In this work, we focus on the propagation properties of optical modes supported at the free surface of a one-dimensional photonic crystal. The contributions of intrinsic and extrinsic loss mechanisms are discussed. The developed understanding is applied to the design of structures that are optimized to support long propagating optical surface waves. We experimentally demonstrate, for the first time, the existence of optical surface waves capable of propagating over centimeter-scale distances in the visible spectral range. This result opens new perspectives for the use of optical surface waves in integrated optics and for light-matter interactions at interfaces.

Optical surface waves are electromagnetic modes that can exist and propagate along the interface separating two distinct media. They have raised a great interest in the past decades because of the large field concentration achievable in the vicinity of the surface, which can be used for enhanced light-matter interactions.

While the existence of a guided mode might be permitted between two interfaces under the sole condition of total internal reflection, total internal reflection alone is not sufficient to create the conditions for light confinement along a single interface. The conditions required for the existence of an optical surface mode are rather strict in terms of materials and geometries and their occurrence is limited to a few identified cases so far [1].

Currently, optical surface waves can be divided into two main families: surface polaritons and “dielectric” surface waves. This distinction is made based on the polarizability of the material on which they occur. Surface polaritons can exist when an incident electromagnetic field is able to couple significantly to a highly polarizable field or its associated physical species [2], such as plasmons, excitons or phonons. The most common example is probably the well-known surface plasmon polaritons (SPPs) where an electromagnetic radiation couples to surface-charge oscillations at a metallic interface. For a such metal-bound electromagnetic mode, the major loss occurs due to free electron scattering, which dramatically limits the propagation length to distances of the order of 10 – 100 μm in the visible [3]. While SPPs have found a variety of practical applications ranging from ultra-sensitive biochemical detection [4], to subwavelength microscopy [3,5], and nanomanipulation [6] their practical application to integrated optics is restricted by the short propagation length they offer. This important constraint has motivated the investigation of more advanced concepts such as the so-called long-range surface plasmon polaritons. This type of mode is proven to propagate over greater distances than standard SPPs [7,8] but comes at the price of a quite limiting geometry. The longest reported value in the visible is in millimeter range [9].

Optical surface modes have also proven to exist between two lossless dielectric media. The absence of an evident absorption mechanism has motivated several studies to claim or imply that the existence of long propagating modes should be possible [10–12]. Two major types of dielectric surface waves have been demonstrated so far. One type, referred to as Dyakonov surface waves, can exist at the interface between two transparent media where at least one has birefringence properties [13]. Pioneering investigations have been performed on Dyakonov surface waves [1,14], validating their existence and demonstrating propagation over a distance of the order of 1 mm in the visible [15]. The major limitation in working with Dyakonov surface waves lies in the practical complexity inherent to the fabrication of materials with well-controlled birefringence properties. The second type of dielectric optical surface waves includes optical modes that can exist along the interface separating a one-dimensional photonic crystal from a homogeneous dielectric medium [16,17]. They are often referred to as Bloch surface waves (BSWs). Surface confinement is ensured by multiple scattering within the photonic crystal in this case. These modes are of particular interest because they can be supported by structures that are readily compatible with standard thin film technologies. The operational wavelength of a Bloch surface mode can be easily tuned by carefully selecting the materials and the layer thicknesses of the one-dimensional photonic crystal. BSWs have been observed over a broad spectral range spanning from near-UV to mid-infrared [18–22]. While structures displaying a propagation length of the order of a few hundred microns at visible wavelengths [23] and around one millimeter at telecom wavelengths [19] have been reported, no particular efforts have been carried out to describe the underlying loss mechanisms, nor to provide an estimate of propagation lengths that one might realistically achieve. The low-loss hypothesis of dielectric surface waves still remains speculative at this point [11].

This work focuses on the propagation properties of BSWs as a potential candidate for optical operations on a chip scale. A discussion of the different loss mechanisms of BSWs is presented, considering both intrinsic and extrinsic factors. In this discussion, the primary role of free radiation into the substrate as a key contribution to the losses is hypothesized. An eigenmode solver-based one-dimensional model is developed to study this hypothesis. The 1D model is then used to design structures that are optimized to support a long propagating surface mode. In order to validate our assumption, the designed structures are fabricated with a technique capable of providing a high surface quality. A record propagation length of 1.4 cm in the visible spectral range is experimentally measured. This value sets a new benchmark for optical surface waves.

Bloch surface modes are characterized by a mode profile that is exponentially decaying, both in the superstrate medium – in this case air – and in the one-dimensional photonic crystal structure. More precisely, the periodic nature of the stratified medium imposes a periodic evolution of the field within the structure, modulated by an exponentially vanishing envelope. The maximum of the field is located near the interface, but within the top most layer of the structure. A typical field distribution of a Bloch surface mode can be seen in Fig. 1(a). In this case, the one-dimensional photonic crystal consists of a stack of $N = 10$ lattice periods. The lattice consists of Ta_2O_5 and SiO_2 layers with respective thicknesses of 107 nm and 158 nm. The periodicity of the stack is interrupted by an additional 34 nm thin Ta_2O_5 defect layer. This structure supports a TE-polarized surface mode.

The dispersion curve of the optical surface mode is computed using the CAvity Modelling FRamework (CAMFR) eigenmode solver [24]. It is shown as a red line in the dispersion diagram of Fig. 1(b). The mode dispersion extends from the air line to the SiO_2 line (indicated as black solid lines), which it finally intersects. The region located between these two lines constitutes the “historical” working range of BSWs because the surface mode can be excited from the substrate side using a Kretschmann-like configuration [25]. For a given lattice, the position of the dispersion curve is mostly dictated by the parameters of the top most layer terminating the structure.

In this work, three main loss mechanisms that might limit the propagation length of Bloch surface waves are envisaged: (i) Radiation into the substrate. The dispersion line of the mode is mostly located above the fused silica substrate (SiO_2) line. This means that energy propagating in the mode within this range of frequencies can freely couple to the substrate assuming that the parallel component of the wavevector is conserved. Bloch surface modes above the SiO_2 line are thus inherently radiating modes. The magnitude of this loss can be intuitively understood as being dictated by the overlap of the surface mode with the radiation continuum. Increasing the number of lattice periods that physically isolate the surface mode from the substrate should thus decrease its impact. This loss mechanism is intrinsic to the nature of the mode. (ii) Light scattering induced by the surface roughness and layer defects. The amount of scattering is related to the quality of the fabrication and thus, is extrinsic to the surface mode. (iii) Material absorption. A large fraction of the mode is located within the periodic structure, and propagation takes place perpendicular to the periodicity. Materials used in thin film technologies are usually characterized for, and with, an illumination at normal incidence. While nanometer to micron thick layers of material might not display any significant absorption, even minor residual absorption levels might become problematic when aiming at long scale in plane propagation. This loss mechanism is extrinsic to the surface mode and might ideally be tailored by appropriate choice of the materials.

An ideal structure that would consist of lossless dielectric materials and perfect interfaces, i.e. free from any extrinsic loss mechanism, should only be limited by the authorized radiation through the substrate.

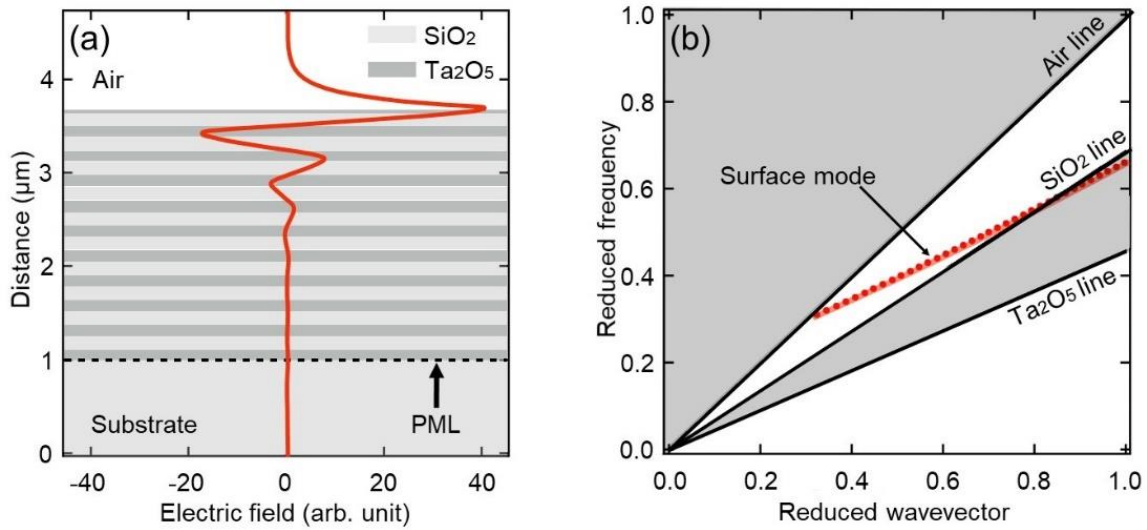


FIG. 1. (a) Calculated distribution of the transverse electric field for a TE-polarized Bloch surface mode at a wavelength of 633 nm. (b) Dispersion diagram of the surface mode presented in Fig 1(a). The x and y axis are reported in reduced unit: reduced wavevector $k_{\text{red}} = \frac{k a}{2\pi}$ and reduced frequency $\omega_{\text{red}} = \frac{\omega a}{2\pi c}$ where a is the lattice period of the structure. The dispersion curve of the surface mode is shown as red dots. It extends from the air line on the low reduced frequency side to the SiO_2 line and beyond as the reduced frequency increases.

We use a 1D model to evaluate the impact of radiation losses. Leakage radiation can be elegantly simulated by using a perfectly matched layer (PML) boundary condition, that acts as a perfect absorber at the interface between the surface mode and the mode continuum of the substrate. The complex propagation constant of the surface mode is calculated as the output of the model $k_{\text{BSW}} = k_{\text{real}} + i k_{\text{im}}$. The layers are modeled as perfect interfaces of lossless materials, and thus any technology-related loss is excluded. The model is expected to give an upper limit for the propagation losses of BSWs. Conventionally, the propagation length of a mode is calculated as the distance where the mode intensity decays by a factor of $1/e$, in analogy to Beer-Lambert's law. Following this analogy, it is common to relate the absorption

coefficient α , to the imaginary part of the wavevector k_{im} (see [2]). The propagation length can then be written as: $L_{BSW} = \frac{1}{\alpha} = \frac{1}{2 k_{im}}$.

The imaginary wavevector of a surface mode, for a given multilayer structure, can then be fed into a simple optimization process. Structures supporting modes with minimal losses can thus be designed (see Supplementary Information). Figure 1 (a) and (b) correspond to the field distribution and dispersion diagram of a structure that is optimized for long propagation and large surface electric field simultaneously.

The propagation length of a one-dimensional photonic crystals having identical lattice parameters as the structure shown in Fig.1, but with a number of lattice periods ranging from 2 to 10 are computed (see Fig S1(a) in Suppl. Info.). Each computation takes only a few seconds using a personal computer. Assuming thus that radiation into the substrate is the only limiting mechanism, it is found that a structure with 4 lattice periods should be enough to ensure a propagation length greater than 200 μm . Furthermore, it indicates that a structure consisting of 7 lattice periods, fairly reasonable in terms of fabrication, should enable the propagation of a surface mode over 4 cm. It is also worth noticing that propagation over 1 m could be achieved with a technologically acceptable 10 lattice periods structure.

In order to experimentally validate our assumptions, a set of multilayer stacks with identical structural parameters but increasing number of lattice periods, from 4 to 7, is fabricated. An important part of this study relies on the capacity to isolate the losses induced by the predicted, intrinsic, radiation into the substrate from the two other extrinsic mechanisms. Ion beam sputtering technique is used to deposit the thin film multilayer structures and ensure high surface quality and low material absorption (see part II in Suppl. Info.).

The fabricated structures are characterized using a specifically assembled setup operating in a Kretschmann-type coupling configuration. As a first step, the angle at which a 633 nm radiation couples to the surface mode is measured. According to our eigenmode computations, coupling into the surface mode is expected to occur at an angle of 63.6°. Experimentally, excitation of the optical surface mode is observed for an incident angle of 63.9° \pm 0.5°. This very good agreement with the numerical predictions validates the precision of the layer deposition process. Figure 2(a) shows a set of optical micrographs aggregated in a stack. Each micrograph corresponds to the optical image of the propagating surface wave acquired on each of the four samples fabricated. The image stack is assembled such that all the surface wave coupling points, where the excitation beam intersects the surface plane, are vertically aligned along the $d = 0$ line. The images are shown in false colors. The scale bar corresponds to a distance of 2 mm. The influence of the number of lattice periods can be clearly visualized on this figure. In particular, it is possible to observe that, starting from $N = 6$, the propagation of the surface wave extends over distances greater than 2 mm. In the case of the structure with 7 periods, the propagation extends well beyond the drawn 1 cm line.

Figure 2(b) shows the relative intensity decay profile of each sample. The latter is obtained by averaging the scattered intensity recorded in ten distinct positions of the sample to get rid of the effect of local scattering centers. The intensity variation is reported in dB, while the distance on the x-axis is reported in millimeters. Black dashed lines are added and serve as guide for the eyes. The propagation loss in dB/mm can be determined for each sample by directly measuring the decay per distance unit. The associated propagation length is reported in Fig 3. The strong reduction of the propagation losses when increasing the number of lattice period is clearly visible. The associated increase in propagation length predicted by our 1D eigenmode model is also confirmed qualitatively. A record propagation length of 14 mm is achieved for the structure consisting of 7 lattice periods. This figure surpasses by over one order of magnitude the longest optical surface wave previously reported in the visible. More specifically, it is over 2 orders of magnitude greater than figures achieved with standard SPPs, and 1 order of magnitude greater than the longest propagation achieved with Dyakonov

surface waves and long-range surface plasmon polaritons, at equivalent optical frequencies. It is also interesting to notice that the 7-period structure has an attenuation figure estimated to 0.3 dB/mm. This figure constitutes a significant milestone. It places optical surface waves close to the range of what is reported for planar waveguides at visible wavelength, which are typically 0.01 to 0.1 dB/mm (see for example [26–28]). This result demonstrates that dielectric optical surface waves have the potential to transport optical information on a chip scale, while being noticeably more sensitive than guided waves to active or passive surface modifications. This last point offers room for development of more efficient and more compact sensors, detectors, or electro-optical modulators, for example.

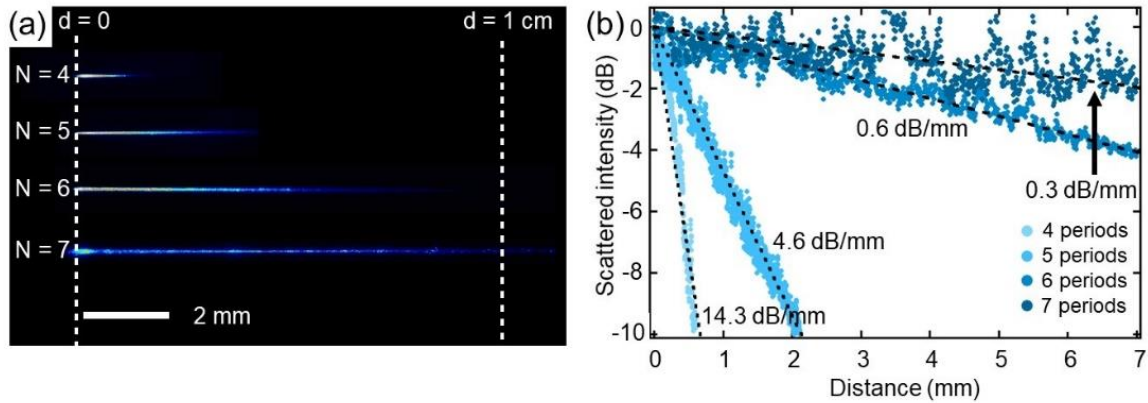


FIG. 2. (a) Images of the propagating BSWs (false colors) (b) Scattered intensity profile as a function of the distance from the injection point for each of the four fabricated samples.

As a separate validation, the propagation lengths of structures with a number of lattice periods ranging from 2 to 6 are computed using a rigorous time domain solver (see part IV in Suppl. Info.). Computation times significantly increase from a few minutes for the 2-period structure to a few days for 6 periods. Larger structures have not been calculated because of the too long computation time.

The calculated propagation lengths obtained using the two numerical methods are reported as a function of the number of lattice periods in Fig. 3 along with the experimental data (red dots). Two main observations can be made. First, a fair agreement can be observed between the two numerical methods. There is as well a good agreement between the two numerical methods and the experimental data. This point validates our simple approach of introducing a perfectly matching layer acting as a perfect absorber in order to mimic the radiation losses in our 1D eigenmode solver-based model. As one could expect, the purely 1D eigenmode calculations provide slightly more optimistic predictions than the 3D time domain calculations. Nevertheless, the use of our 1D approach over the 3D time domain method is a significant gain in terms of modelling complexity and comes with a significant benefit: calculations times are reduced from days to seconds and, as a consequence, rapid iteration cycles and optimizations can be performed.

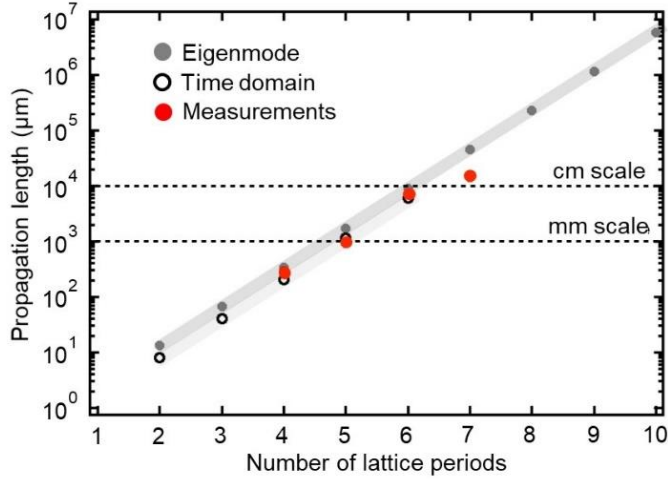


FIG. 3. Comparison between the experimental and numerical propagation lengths as a function of the number of lattice periods in the multilayer structure.

The experimental measurements precisely follow the numerical predictions obtained with the two independent methods, up to $N = 6$. The results shown in Fig. 3 thus validate the prediction of exponential increase of the propagation length with the number of lattice periods (see Fig. S1(a) in the Suppl. Info.), and our initial hypothesis that the major loss mechanism corresponds to the radiation of light through the multilayer. For the structure having 7 periods however, a discrepancy between the predicted (4.5 cm) and the measured (1.4 cm) propagation length appears. The nature of this discrepancy has not been identified at this point. It could possibly be attributed to a saturation of the exponential trend, which causes another loss mechanism to become dominant. Scattering, whether along the top surface or at layer interfaces, as well as residual material absorption, might be intuitively considered. For example, a set of early calculations based on the 1D model shows that material absorption levels of the order of $\text{Im}(n) = 10^{-5}$, which are below our measurement capabilities, could be consistent with the observed saturation. More importantly, this observation tends to indicate that any attempt to further improve the propagation length of BSWs in the visible might require an important effort to further control the surface quality and the residual coating material absorption. It might also be of interest to investigate the impact of scattering at the interfaces by replacing the standard fused silica wafers used in this experiment with superpolished substrates. The substrate roughness, before deposition, would then be reduced from the nanometer to ångström levels thus potentially significantly the associated scattering contribution.

Another interesting point can be raised from this study. The results presented here demonstrate that leakage radiation limits the propagation of a carefully designed and fabricated structure supporting a Bloch surface mode at (k, ω) coordinates located in between the air line and the substrate line. It might thus be of great interest to investigate the propagation properties of Bloch surface modes being operated beyond the substrate line, that is, where radiation of the surface mode into the substrate is simultaneously prohibited by multiple scattering and by total internal reflection. In this region, where $w_{\text{red}} < \frac{k_{\text{red}}}{n_{\text{substrate}}}$ (here in between the SiO_2 line and the Ta_2O_5 line), the field is confined nearer to the surface and no radiation into the substrate is allowed. It is expected that a mode operated in this region (non-radiating regime) exhibits a propagation length equivalent to that of a mode operated in the radiating regime despite fewer lattice periods (e.g. 3 instead of 7). Such a structure would, on one hand, benefit from a simpler fabrication process and possibly from reduced number of fabrication-related defects and layer strain. On the other hand, the greater magnitude of the wavevector in this region prohibits the use of a Kretschmann-type excitation scheme, and thus imposes the use of another coupling scheme, e.g. a grating coupler.

In conclusion, we have demonstrated, for the first time, the existence of optical surface waves that propagate over a centimeter-scale at visible wavelengths. We have focused our study on Bloch surface waves which are supported at the surface of a one dimensional photonic crystal. We report a 1.4 cm propagation length for a structure comprising of 7 lattice periods. This figure is an order of magnitude greater than the longest reported value for Dyakonov surface waves and long-range surface plasmon polaritons, and two orders of magnitude greater than standard surface plasmon polaritons. We validated that the propagation length in carefully fabricated structures operated above the substrate line must only depend on the surface mode overlap with the radiation continuum in the substrate. Our results open new perspectives for the use of optical surface waves for in-plane optical distribution and processing of information. In particular, it might motivate further work on the on-chip interfacing of Bloch surface states with other optical surface states.

The authors acknowledge Raphaël Monnard for the AFM measurements of the samples. The work of Nicolas Descharmes and Raphaël Barbey is supported by the Gebert Rüt Stiftung, project number GRS 019/16.

*bala@dtu.dk

- [1]O. Takayama, L. Crasovan, D. Artigas, and L. Torner, *Phys. Rev. Lett.* **102**, 043903 (2009).
- [2]C. F. Klingshirn, *Semiconductor Optics* (Springer Science & Business Media, 2012).
- [3]W. L. Barnes, A. Dereux, and T. W. Ebbesen, *Nature* (2003).
- [4]A. V. Kabashin, P. Evans, S. Pastkovsky, W. Hendren, G. A. Wurtz, R. Atkinson, R. Pollard, V. A. Podolskiy, and A. V. Zayats, *Nature Materials* **8**, 867 (2009).
- [5]M. Specht, J. D. Pedarnig, W. M. Heckl, and T. W. Hänsch, *Physical Review Letters* **68**, 476 (1992).
- [6]M. L. Juan, M. Righini, and R. Quidant, *Nature Photonics* **5**, 349 (2011).
- [7]P. Berini, *Advances in Optics and Photonics* **1**, 484 (2009).
- [8]D. Sarid, *Physical Review Letters* **47**, 1927 (1981).
- [9]V. N. Konopsky and E. V. Alieva, *Phys. Rev. Lett.* **97**, 253904 (2006).
- [10]L. Yu, E. Barakat, T. Sfez, L. Hvozdar, J. Di Francesco, and H. Peter Herzig, *Light Sci Appl* **3**, e124 (2014).
- [11]M. Menotti and M. Liscidini, *JOSA B* **32**, 431 (2015).
- [12]X. Lei, Y. Ren, Y. Lu, and P. Wang, *Phys. Rev. Applied* **10**, 044032 (2018).
- [13]M. I. D'yakonov, *Zh. Eksp. Teor. Fiz* **67**, (1988).
- [14]D. Artigas and L. Torner, *Phys. Rev. Lett.* **94**, 013901 (2005).
- [15]O. Takayama, D. Artigas, and L. Torner, *Nature Nanotechnology* **9**, 419 (2014).
- [16]P. Yeh, A. Yariv, and C.-S. Hong, *J. Opt. Soc. Am.*, *JOSA* **67**, 423 (1977).
- [17]P. Yeh, A. Yariv, and A. Y. Cho, *Applied Physics Letters* **32**, 104 (1978).
- [18]G. M. Smolik, N. Descharmes, and H. P. Herzig, *ACS Photonics* **5**, 1164 (2018).
- [19]R. Dubey, E. Barakat, M. Häyrynen, M. Roussey, S. K. Honkanen, M. Kuittinen, and H. P. Herzig, *J. Eur. Opt. Soc.-Rapid Publ.* **13**, 5 (2017).
- [20]W. M. Robertson and M. S. May, *Applied Physics Letters* **74**, 1800 (1999).
- [21]R. Wang, H. Xia, D. Zhang, J. Chen, L. Zhu, Y. Wang, E. Yang, T. Zang, X. Wen, G. Zou, P. Wang, H. Ming, R. Badugu, and J. R. Lakowicz, *Nature Communications* **8**, 14330 (2017).
- [22]R. Badugu, J. Mao, S. Blair, D. Zhang, E. Descrovi, A. Angelini, Y. Huo, and J. R. Lakowicz, *The Journal of Physical Chemistry C* **120**, 28727 (2016).
- [23]I. V. Soboleva, E. Descrovi, C. Summonte, A. A. Fedyanin, and F. Giorgis, *Applied Physics Letters* **94**, 231122 (2009).
- [24]P. Bienstman, *Rigorous and Efficient Modelling of Wavelength Scale Photonic Components*, Ghent University, 2001.
- [25]E. Kretschmann and H. Raether, *Zeitschrift Für Naturforschung A* **23**, 2135 (1968).
- [26]D. H. Hensler, J. D. Cuthbert, R. J. Martin, and P. K. Tien, *Appl. Opt.*, *AO* **10**, 1037 (1971).

- [27]A. Gorin, A. Jaouad, E. Grondin, V. Aimez, and P. Charette, *Opt. Express*, OE **16**, 13509 (2008).
- [28]J. D. B. Bradley, C. C. Evans, F. Parsy, K. C. Phillips, R. Senaratne, E. Marti, and E. Mazur, in *2010 23rd Annual Meeting of the IEEE Photonics Society (2010)*, pp. 313–314.

Supplementary Information for:

Optical surface waves on one-dimensional photonic crystals: investigation of losses mechanisms and demonstration of centimeter-scale propagation

Babak Vosoughi Lahijani,^{1,2,*} Nicolas Descharmes,¹ Raphael Barbey,¹ Gael D. Osowiecki,¹ Valentin J. Wittwer,³ Olga Razskazovskaya,³ Thomas Südmeyer,³ and Hans Peter Herzig¹

¹ Optics & Photonics Technology (OPT) Laboratory, École Polytechnique Fédérale de Lausanne (EPFL), rue de la Maladière 71b, CH-2002 Neuchâtel, Switzerland

² Currently with the Department of Photonics Engineering, DTU Fotonik, Technical University of Denmark, DK-2800 Kgs. Lyngby, Denmark

³ Laboratoire Temps-Fréquence, Université de Neuchâtel, Av. de Bellevaux 51, CH-2000 Neuchâtel, Switzerland

I. Design routine of long propagating optical surface waves

The design routine relies on three main parameters, which are: (i) the lattice parameters of the periodic structure, (ii) the number of lattice periods, and (iii) the thickness of the top most layer. The lattice parameters are chosen based on the materials used for the layer deposition, and more specifically, based on their refractive indices. The optimization process first establishes rough lattice parameters depending on the desired operation wavelength. The thickness of the top most layer is then chosen such that a satisfying trade-off is achieved between (i) the level of confinement of the field at the interface of the multilayer and the top medium (air), (ii) the calculated propagation length, and (iii) the coupling angle required to couple to the surface mode through a prism. The structure is designed to operate around a central wavelength of 633 nm. The calculated coupling angle for this structure is 63.6° in a fused silica prism at 633 nm which corresponds to an angle of 72.5° in air using a right-angle prism.

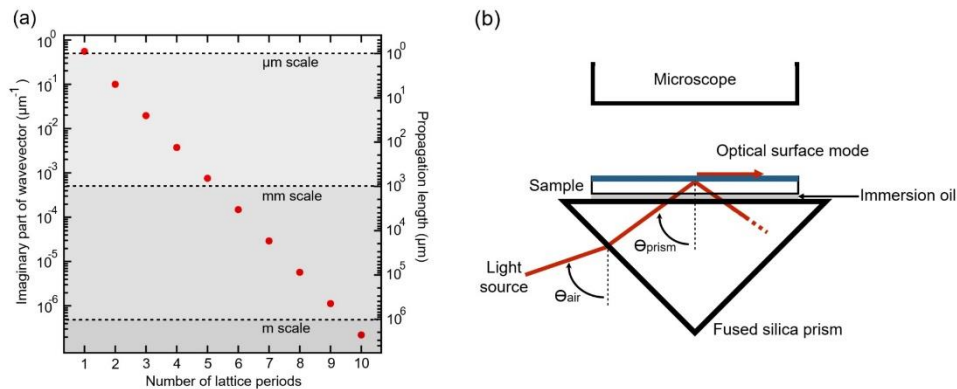


FIG. S1. (a) Imaginary part k_{im} of the wavevector and associated propagation length calculated using eigenmode solver (CAMFR) of the Bloch surface mode as a function of the number of periods. Both quantities are plotted on a logarithmic scale. The simulation predicts an exponential increase of the propagation length when the number of periods is increased. This prediction is consistent with a decrease of the surface mode overlap with the radiation continuum, assuming that no other loss mechanism becomes predominant. (b) Schematic of the experimental apparatus used to characterize the fabricated structure. Excitation of the surface mode is performed at a controlled angle through a fused silica prism and index matching oil. Propagation of the surface mode is confirmed and monitored using a specifically assembled microscope located above the investigated structure.

Figure S1(a) shows the computed evolution of the imaginary part k_{im} , and the corresponding propagation length, when the number of lattice periods is increased from 1 to 10. The plot is

shown on a semilogarithmic scale. An intuitive exponential decrease of the loss term k_{im} can be observed as the number of lattice periods increases. The latter corresponds to a vanishing of the overlap between the surface state eigenmode and the radiation continuum. This effect is accompanied by an exponential increase of the theoretical propagation length of the mode.

II. Thin film multilayer deposition using ion beam sputtering technique

An ion beam sputtering machine (Navigator 1100, CEC GmbH) is used to produce the thin film multilayer structures and ensure high surface quality and low material absorption. Xenon is used as the sputtering gas. According to the designed structure, tantalum pentoxide (Ta_2O_5 , $n = 2.16$ at $\lambda = 633$ nm) as high-refractive index and silicon dioxide (SiO_2 , $n = 1.49$ at $\lambda = 633$ nm) as low-refractive index material are used. Ellipsometric combined with transmission measurements are performed on layers of the two materials in order to precisely assess the refractive indices and absorption coefficients of each material. The measurements indicate that no absorption is measurable on any of them, down to a level of $\text{Im}(n) = 10^{-4}$ (imaginary part of the refractive index) which is the minimum detectable quantity. The oxides are formed by oxidation of metallic Ta and Si released from the sputtering targets with a deposition rate of about 0.1 nm/s. During the deposition, the vacuum pressure does not exceed $2 \cdot 10^{-3}$ mbar and the substrates are heated to 150 °C. The automated coating process is precisely controlled by broadband optical monitoring. The quality of the surface is assessed using an atomic force microscope (AFM). The average roughness of the surface is found to be 1 nm.

III. Experiment

A schematic of the excitation and monitoring part is shown on Figure S1(b). Excitation of the surface modes is performed using a Kretschmann-type configuration based on a 45° fused silica prism and a goniometer. The light source consists of a supercontinuum source from NKT Photonics equipped with a custom acousto-optical tunable filter. The light source emission is centered around 633 nm with a 1.5 nm bandwidth. The polarization of the light is controlled using a polarizer and coupled into a polarization maintaining fiber. The polarized light is first collimated and then refocused using a 100 mm focal length lens through the prism onto the surface of the BSWs platform. The propagation length of the optical surface mode at the surface of the multilayer is measured with a custom microscope detection system. The latter collects the residual light that is scattered from the surface as the surface mode propagates. Imaging is performed using a high sensitivity scientific CMOS camera (Hamamatsu Orca Flash 4 V2). The measurement of the intensity profile, and the determination of the decay constant, is complicated by the presence of local variations in the scattered intensity induced by localized surface defects. To circumvent this issue, ten different acquisitions are performed, for each sample, in ten different locations of the surface. The ten images are then summed together which leads to a strong reduction of the noise. The resulting image is used to retrieve the decay constant.

IV. 3D time domain simulation

To model the propagation lengths of the designed structures using a rigorous time domain solver (CST Microwave Studio), a perfectly matching layer (PML) boundary condition is applied to the exterior boundaries. The multilayer is illuminated using a Gaussian beam at the designed coupling angle. The fields that radiate through the substrate reach the PML where they are absorbed. No material absorption or surface roughness effects is considered in this model to mimic the computations performed using our eigenmode-based model. A decay of the electromagnetic field intensity is observed along the propagation of the surface mode and, here again, the calculated propagation length corresponds only to the radiation loss through

the multilayer. The rigorous time domain modeling is greatly time-consuming, particularly for longer propagation lengths. For this reason, time domain calculations have only been performed for multilayers with up to 6 layer pairs.